GANITA,Vol.72(2), 2022, 127-151

STUDY OF EFFECT OF VARIOUS SHAPES OF NANOPARTICLES IN CATHETERIZED ARTERY WITH ELLIPTICAL STENOSIS : COMPARING ANALYTICAL AND NUMERICAL SOLUTION

R. BALI and B. PRASAD

Abstract

Recent developments in the field of nanotechnology for novel haematological treatments has higher scopes and befitting results.Owing to such neoteric outcomes the problem of nanoparticles in a catheterized artery with elliptical stenosis has been addressed here. A theoretical model having permeable walls, treating blood as a base fluid for various shapes of nanoparticles suspended, is presented for the same. The disposition of blood is described to be that of a viscous nanofluid. The calculations are executed under mild stenosis conditions. The nanoparticles of shapes like bricks, platelets, cylinders and blades are considered. Hamilton-Crosser model is applied to attain expression for thermal conductivity. Thermophysical properties like specific heat capacity and thermal expansion have also been considered. The exact solution is obtained using Cauchy- Euler method. The numerical solution is also obtained for the same using finite difference scheme and both the solutions have been compared. Also, the existence and uniqueness of the exact solution is given using Green's theorem. The effects of shape of nanoparticles, volume fraction, Grashof number, Darcy number, stenosis height and heat source parameter have been depicted graphically on temperature and velocity of nanofluid. A major assessment states that platelets shaped nanoparticles show maximum rise in temperature and velocity while brick shaped nanoparticles show minimum rise in temperature and velocity. This mathematical model has relevance in nano-drug delivery in the therapeutics of cardiovascular diseases.

2010 *Mathematics subject classification:* primary 00A69, 92B10; secondary 35Q09, 46N20.

Keywords and phrases: Stenosis, Catheter, Nanoparticles, Heat source parameter, Hamilton-Crosser model, Darcy number, Grashof number, Green's theorem.

1. Introduction

Cardio vascular diseases are a paramount cause of deaths all over the world. An exceedingly transpiring cardiovascular ailment is atherosclerosis. It is the build out of stenosis or blockages as the outcome of deposition of fatty materials in the inner lining of the artery. Such occlusions cause reduction in artery's cross section which in turn causes insufficient blood supply to the body. The hemodynamic context of the arteries is a salient discipline of analysis under stenotic circumstances [1] [2]. The experimental data available to design mathematical models will be highly useful to develop better

aids and devices to restrict mortality rates due to various cardio vascular diseases.

Stenosis is the development of plaques, fats or cholesterol that lessens the blood flow through arteries. The burgeoning of such depositions in arteries may arise at one or more sites that can cause infraction, ischemic stroke, sporadic blood flow rate etc. Catheter is a widely employed medical method in contemporary medicine for treating atherosclerosis. This diagnostic tool holds resemblance to an empty cylinder having a narrow radius which is inserted into the artery. Catheter is composed of medical grade polyvinyl chloride or polyester constructed thermoplastic polyurethane etc. [4]- [6]. The infixing of catheter largely effects the hemodynamic in the vicinity of stenosis in the artery. Abundant mathematical inspections have been carried out to diagnose the consequences of stenosis on the blood flow under catheterized conditions.[7]-[12].

Kamangar et al [13] gave the numerical investigation of the effect of stenosis geometry on the coronary diagnostic parameters. They showed that elliptical shaped stenosis has the highest resemblance with the functional severity in an actual artery stenosis. Thus, the study of elliptical shaped artery stenosis will have a wider and more practical application in the treatment of cardiovascular diseases.

The last decades have witnessed a revolution in the field of biomedical sciences with the utilization of nanotechnology. The manipulation of nanotechnology is grounded on the materials with dimensions of about 100 nm or lower. Such particles have sizes lying in the range of cell which provide a better interaction with them.[14]. Diverse medical modalities like drug delivery and cancer therapy have effectively been carried out with the use of nanotechnology in biological systems [15]. Richard P. Feynman was the first to introduce nanoscience and nanotechnology and science then there has been an immense revolution in the field [16][17].

The nano-based medical strategies are being increasingly used because they can effectively control drug delivery systems. Nanodrugs can be easily integrated through diverse non-covalent and covalent adsorptions on their outer membrane [18]. These provide myriad options for the suitable designing of drugs of various geometries for their specific targeting. Some nanocarriers may carry more than one drug likewise for diagnostics and therapeutics, collectively called theranostic platform. Thus, different nanoparticles have exhibited promising application in the field of treatment of various cardio vascular diseases.

Ellahi et al [19] analysed spherical nanoparticle behaviour in arteries with composite stenosis and permeable walls. Nadeem and Ijaz [20] [21] mathematically studied spherical nanoparticles possessing drug in stenosed artery simultaneously slip effects on the arterial wall. Chatterjee et al [22] deployed Bernstein polynomial estimation to analyse the effects of nanofluids in a stenosed artery. Rathore and Srikanth [23] considered blood as a micro-polar nanofluid in an artery with stenosis in the influence

of a catheter.

When nanoparticles are added to a fluid, the temperament of the system depends on their thermophysical responses and the shape of nanoparticles [24]. Heat transfer in blood vessels occurs mainly via convection, the efficiency of which resorts to the thermophysical amputations of the nanofluid [25]. Nanoparticles have displayed very high thermal conductivities. Thus, the study of nanofluid thermophysical attributes have a stupendous significance in engineering nano-drug based therapies for the treatment of cardiovascular diseases.

Also, the nanoparticle disposition is a noteworthy nanoparticle norm. Nanoparticles of different shapes either occur naturally or are engineered. Various nanoparticles configurations have different schemes of applications. Sastry et al[26] studied the drug delivery in cardio vascular circulation considering unsteady micropolar nanfluid flow. Moitoi and Shaw [27] also analysed nanoparticle based drug targeting for the treatment of cardiovascular diseases. Most of the studies conducted have considered spherical shaped nanoparticles. Notwithstanding the fact that they have not much feasibility. Drug delivery, clinical diagnosis, cancer therapy has a utilization of non-spherical shaped nanoparticles [28]. Discernibly, nanoparticles of shapes like brick, platelet, blade and cylinder etc have tremendous prominence in drug delivery. Timofeeva et al [29] gave an experimental analysis of the effects of studied thermal conductivity and viscosity on various geometries of nanoparticles. Samantaray et al [30] studied the effects of different shapes of nanoparticles and also focused on their heat transfer.Shaw et al [31] theoretically analysed the effects of drug carrier geometry for nanoparticle based drug delivery in a micro vessel.

Motivated by these researches, this mathematical work is consigned to probe into the consequence of various geometries of nanoparticles in an artery having elliptical stenosis with a catheter. The equation of continuity, Navier-stokes equation and heat diffusion equations are implemented to scheme the mathematical model. The exact solution for temperature and velocity is solved using Cauchy- Euler method. The existence and uniqueness of the exact solution is proved using green's theorem. Numerical solution is also obtained for the same using finite difference method using MATLAB. The obtained analytical and numerical solutions have been compared. The influences of shape parameter, volume fraction, heat source parameter, stenosis height, Grashof number and Darcy number have been displayed graphically on temperature and velocity of nanofluid in the stenosed artery. This model has an application in the treatment of blockages in arteries with the use of nanoparticles.

2. Mathematical Formulation

Steady and laminar flow of blood in a cylindrical artery of length L has been considered. The incompressible flow in the artery is modelled using cylindrical

co-ordinates.Let the velocity vector be $(u^{'}, v^{'}, w^{'})$here $u^{'}$ is in $z^{'}$ direction, $v^{'}$ is along radial direction or $r^{'}$ direction and $w^{'}$ is along $\theta^{'}$ direction. For the case of axis-symmetricity $w^{'} = 0$, since $\theta^{'}$ represents the circumferential direction. The configuration of elliptical stenosis [13] is defined as:-

$$R'(z') = \begin{cases} R_0 - \frac{\delta'}{R_0} \sin \pi(\frac{z'-d'}{L}); & d' \leq z' \leq d' + L_0 \\ R_0; & otherwise \end{cases} \tag{2.1}$$

where $d^{'}$ represents location of stenosis, $L_0^{'}$ is length of the stenosed part, $L^{'}$ is arterial length, R_0 is radius of normal artery and $R^{'}(z^{'})$ is arterial radius with stenosis.R_c is catheter's radius.

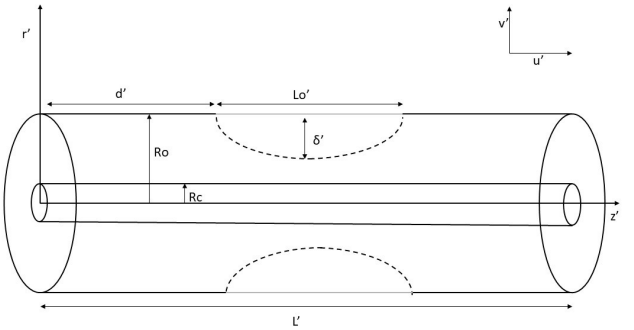

Figure 1. Geometrical representation.

Equation of continuity in cylindrical co-ordinates :

$$\frac{\partial \rho_{nf}}{\partial t'} = \frac{1}{r'} \frac{\partial r \rho_{nf} v'}{\partial r'} + \frac{1}{r'} \frac{\partial \rho_{nf} w'}{\partial \theta'} + \frac{\rho_{nf} w'}{\partial z'} = 0 \tag{2.2}$$

Navier-Stokes equation in cylindrical co-ordinates:

$$\begin{aligned} &\frac{\partial v'}{\partial t'} + v' \frac{\partial v'}{\partial r'} + \frac{w'}{r'} \frac{\partial v'}{\partial \theta'} - \frac{w'^2}{r'} + u' \frac{\partial v'}{\partial z'} = F_{r'} - \frac{1}{\rho_{nf}} + \frac{\partial p'}{\partial r'} \\ &+ \frac{\mu_{nf}}{\rho_{nf}} (-\frac{v'}{r^2} + \frac{1}{r'} \frac{\partial}{\partial r'} (r' \frac{\partial v'}{\partial r'}) + \frac{1}{r'^2} \frac{\partial^2 v'}{\partial \theta'^2} + \frac{\partial^2 v'}{\partial z'^2} - \frac{2}{r'^2} \frac{\partial w'}{\partial \theta'}) \end{aligned} \tag{2.3}$$

$$\begin{aligned} &\frac{\partial w'}{\partial t'} + v' \frac{\partial v'}{\partial r'} + \frac{w'}{r'} \frac{\partial w'}{\partial \theta'} - \frac{v' w'}{r'} + u' \frac{\partial w'}{\partial z'} = F_{\theta'} - \frac{1}{\rho_{nf}} \frac{\partial p'}{\partial \theta'} \\ &+ \frac{\mu_{nf}}{\rho_{nf}} (-\frac{w'}{r^2} + \frac{1}{r'} \frac{\partial}{\partial r'} (r' \frac{\partial w'}{\partial r'}) + \frac{1}{r'^2} \frac{\partial^2 w'}{\partial \theta'^2} + \frac{\partial^2 w'}{\partial z'^2} + \frac{2}{r'^2} \frac{\partial v'}{\partial \theta'}) \end{aligned} \tag{2.4}$$

$$\frac{\partial w'}{\partial t'} + v'\frac{\partial u'}{\partial r'} + \frac{w'}{r'}\frac{\partial u'}{\partial \theta'} + u'\frac{\partial u'}{\partial z'} = F_{z'} - \frac{1}{\rho_{nf}}\frac{\partial p'}{\partial z'} + \frac{\mu_{nf}}{\rho_{nf}}\left(\frac{1}{r'}\frac{\partial}{\partial r'}\left(r'\frac{\partial u'}{\partial r'}\right) + \frac{1}{r'^2}\frac{\partial^2 u'}{\partial \theta'^2} + \frac{\partial^2 u'}{\partial z'^2}\right) \tag{2.5}$$

where F' with different indices represents body forces with respect to different directions.

Heat diffusion equation for temperature in cylindrical co-ordinates:

$$\frac{1}{k_{nf}}\left(\frac{\partial T'}{\partial t'} + v\frac{\partial T''}{\partial r'} + w'\frac{\partial T'}{\partial \theta'} + u'\frac{\partial T'}{\partial z'}\right) = \frac{1}{\rho_{nf}c_{p_{nf}}}\left(\frac{\partial^2 T'}{\partial r'^2} + \frac{1}{r'}\frac{\partial T'}{\partial r'} + \frac{1}{r'^2}\frac{\partial^2 T'}{\theta'^2} + \frac{\partial^2 T'}{\partial z'^2}\right) + \frac{H}{\rho_{nf}c_{p_{nf}}} \tag{2.6}$$

T_c is temperature of wall of catheter and T_0 is temperature of artery. T' is nanofluid temperature. The heat generation or heat absorption parameter is represented by H.Now considering nanofluid model, μ_{nf} represents nanofluid viscosity, k_{nf} is nanofluid thermal conductivity, ρ_{nf} is nanofluid density, γ_{nf} is nanofluid thermal expansion coefficient and $C_{p_{nf}}$ is nanofluid heat capacitance.

The governing equations (2.2) - (2.6) are solved under the following assumptions:

1. Flow is steady, laminar and incompressible.
2. Flow is considered two dimensional.
3. Flow is axisymmetric
4. The radial and azimuthal components of fluid velocity is zero.
5. The axial and azimuthal components of temperature is zero.
6. The heat transfer is considered to take place via diffusion in the catheterized artery.
7. Constant heat source parameter is considered for heat generation/absorption due to catheter insertion.
8. The mild stenosis condition $\delta = \frac{\delta'}{R_0} \ll 1$

The modified equations are given henceforth. The governing equations with regard to nanoparticles are given as: -

$$\frac{\partial v'}{\partial r'} + \frac{v'}{r'} + \frac{\partial u'}{\partial z'} = 0 \tag{2.7}$$

$$\rho_{nf}\left(v'\frac{\partial v'}{\partial r'} + u'\frac{\partial v'}{\partial z'}\right) = -\frac{\partial p'}{\partial r'} + \mu_{nf}\left(\frac{\partial^2 v'}{\partial r'^2} + \frac{1}{r'}\frac{\partial v'}{\partial r'} + \frac{\partial^2 v'}{\partial z'^2} - \frac{v'}{r'}\right) \tag{2.8}$$

$$\rho_{nf}\left(v'\frac{\partial u'}{\partial r'} + u'\frac{\partial u'}{\partial z'}\right) = -\frac{\partial p'}{\partial z'} + \mu_{nf}\left(\frac{\partial^2 u'}{\partial r'^2} + \frac{1}{r'}\frac{\partial u'}{\partial r'} + \frac{\partial^2 u'}{\partial z'^2}\right) + g\rho_{nf}\gamma_{nf}(T' - T_0) \tag{2.9}$$

$$\left(v'\frac{\partial T'}{\partial r'} + u'\frac{\partial T'}{\partial z'}\right) = \frac{k_{nf}}{\rho_{nf}c_{p_{nf}}}\left(\frac{\partial^2 T'}{\partial r'^2} + \frac{1}{r'}\frac{\partial T'}{\partial r'} + \frac{\partial^2 T'}{\partial z'^2}\right) + \frac{H}{\rho_{nf}c_{p_{nf}}} \tag{2.10}$$

where T' is temperature, τ_{nf} is shear stress of nanofluid, $(\rho\gamma)_{nf}$ is thermal expansion of nanofluid and k_{nf} is is nanofluid thermal conductivity in the central region of the arteriole. H is constant heat generation or absorption parameter.T_0 is temperature of the peripheral layer.

Now the respective boundary conditions are defined.

The temperature T_0 is prescribed on the surface of the artery wall.

$$T' = T_0 \ \ at \ \ r' = R'(z') \tag{2.11}$$

The temperature on the surface of the catheter T_c

$$T' = T_c \ \ at \ \ r' = R(c) \tag{2.12}$$

The slip velocity at the wall of artery is given as

$$u' = u'_b \ \ at \ \ r' = R'(z') \tag{2.13}$$

Using Darcy law at the boundary of the artery

$$\frac{\partial u'}{\partial r'} = \frac{\alpha}{\sqrt{k_{nf}}}(u'_b - u'_p) \ \ atr' = R'(z') \tag{2.14}$$

u'_B is the slip velocity of blood and u'_p is the velocity at permeable arterial boundary calculated using Darcy law. α is a dimensionless parameter depending upon the nanofluid and artery. Equation (8) is obtained from the Beavers and Joseph condition [35] for boundary between a free fluid and a porous medium.

$$u'_p = -\frac{k_{nf}}{\mu_{nf}}\frac{\partial p'}{\partial z'} + g\rho_{nf}\gamma_{nf}(T' - T_0) \tag{2.15}$$

$$Using \quad T' = T_0 \ \ at \ \ r' = R'(z')$$

$$therefore, u'_p = -\frac{k_{nf}}{\mu_{nf}}\frac{\partial p'}{\partial z'} \tag{2.16}$$

Regardless of substantial research and analysis, there are not many effective theoretical models to define the nanoparticle thermal conductivity. Maxwell pioneered the Effective Medium Theory (EMT) which was studied to a greater extent by Hamilton and Crosser for non-spherical shaped particles. This model enunciates the thermal conductivity of two components in a solution for non-spherical shaped particles., as the result of conductivity of pure materials, along with their respective compositions

and the manner in which they are dispersed in the solution. Thus, it is applied to calculate the thermal conductivity ((k_{nf}) of nanofluid [33]

$$\frac{k_{nf}}{k_f} = \frac{k_p + (n-1)k_f + (n-1)(k_p - k_f)\phi}{k_p + (n-1)k_f - (k_p - k_f)\phi} \tag{2.17}$$

Where k_f is the thermal conductivity of blood, while k_p is nanoparticle thermal conductivity and ϕ is nanoparticle volume fraction. It uses empirical shape factor $n = \frac{3}{\psi}$, where ψ is the sphericity which is termed as the ratio of equal volumes of the sphere's surface area to the real particle's surface area. The values of n for different shapes of nanoparticles is listed in table 3.
The nanofluid density is expressed as

$$\rho_{nf} = (1-\phi)\rho + \phi\rho_p \tag{2.18}$$

where ρ_f is density of blood and ρ_p is nanoparticle density.
Similarly, nanofluid specific heat capacity [33] is calculated as

$$\rho_{nf} c_{p_{nf}} = (1-\phi)\rho_f c_{p_f} + \phi\rho_p c_{p_p} \tag{2.19}$$

The nanofluid thermal expansion [6] is given as

$$\rho_{nf}\gamma nf = (1-\phi)\rho_f\gamma_f + \phi\rho_p\gamma_p \tag{2.20}$$

where $\rho_f c_{p_f}$ and $\rho_f\gamma_f$ is the specific heat capacity and thermal expansion of blood. $\rho_p c_{p_p}$ and $\rho_p\gamma_p$ is nanoparticle specific heat capacity and nanoparticle thermal expansion.

The nanofluid viscosity [28] is given as

$$\mu_{nf} = (1 + A_1\phi + A_2\phi^2)\mu_f \tag{2.21}$$

where A_1 and A_2 is specific to the shape of nanoparticles in the fluid (Table 2). μ_{nf} is nanofluid viscosity and μ_f is blood viscosity.

The non-dimensional variables are :-

$$\begin{cases} r = \frac{r'}{R_0}, z = \frac{z'}{R_0}, v = \frac{v'}{u_{avg}}, u = \frac{u'}{u_{avg}}, p = \frac{R_0 p'}{\mu_f u_{avg}}, \sigma = \frac{d}{R_0}, R_e = \frac{R_0 u_{avg}\rho_f}{\mu_f}, \\ G_r = \frac{g\gamma_f\rho_f R_0^2(T_c - T_0}{\mu_0\mu_f}, \delta = \frac{\delta'}{R_0'}, h = \frac{HR_0^2}{(T_c - T0)k_f}, \Theta = \frac{(T' - T_0)}{(T_c - T_0)}, Da = \frac{k_f}{R_0^2} \end{cases} \tag{2.22}$$

In equations (2.22), G_r is Grashof number, u_0 is average velocity, R_e is Reynolds number, h is heat source parameter and Da is Darcy number.

The transformed non-dimensional equations (2.7) to (2.10) are stated as:-

$$\frac{\partial u}{\partial z} = 0 \tag{2.23}$$

$$\frac{\partial p}{\partial z}\frac{\mu_f}{\mu_{nf}} = \frac{\partial^2 u}{\partial r^2} + \frac{1}{r}\frac{\partial u}{\partial r} + [(1-\phi) + \phi\frac{\rho_p\gamma_p}{\rho_f\gamma_f}] + (1 + A_1\phi + A_2\phi^2)G_r\Theta \tag{2.24}$$

$$\frac{\partial^2\Theta}{\partial r^2} + \frac{1}{r}\frac{\partial\Theta}{\partial r} + h[\frac{k_p + (n-1)k_f + (n-1)(k_p - k_f)\phi}{k_p + (n-1)k_f - (k_p - k_f)\phi}] \tag{2.25}$$

The geometry of the stenosis (2.1) and the boundary conditions (2.11) to (2.14) in non-dimensional form are:-

$$R(z) = \begin{cases} 1 - \frac{\delta}{R_0}\sin\pi(\frac{z-d}{L}); & d \le z \le d + L \\ 1; & otherwise \end{cases} \tag{2.26}$$

$$\Theta = 0 \quad atr = R(z) \tag{2.27}$$

$$\Theta = 1 \quad atr = \frac{R_c}{R_0} \tag{2.28}$$

$$u = u_B \quad atr = R(z) \tag{2.29}$$

$$\frac{\partial u}{\partial r} = \frac{\alpha}{\sqrt{D_a}}(u_b - u_p)atr = R(z) \tag{2.30}$$

3. Solution

3.1. Analytical solution using Cauchy-Euler method The solution to the equations (2.23) to (2.25) using the boundary conditions (2.27) to (2.30) is obtained analytically by using Cauchy-Euler method as: -

The temperature is given as:-

$$\Theta = \frac{1}{4\,(\ln R(z) - \ln R_c/R_0)}[(4\ln R(z) - \ln R_c/R_0) + h[\frac{k_p + (n-1)k_f - (k_p - k_f)\phi}{k_p + (n-1)k_f + (n-1)(k_p - k_f)\phi}] \tag{3.1.1}$$
$$(R(z)^2(\ln r - \ln R_c/R_0) + r^2(-\ln R(z) + \ln R_c/R_0) + (\ln R(z) - \ln r)(R_c/R_0)^2)]$$

The velocity is given as:-

$$\begin{cases} u = \frac{dp}{dz}\frac{(1+A_1\phi+A_2\phi^2)}{4(\ln R(z)-\ln R_c/R_0)}(r^2(\ln R(z) - \ln R_c/R_0) \\ +R(z)^2(-\ln r + \ln R_c/R_0) + R_c^2(-(1 + A_1\phi + \\ A_2\phi^2)[(1-\phi) + \phi\frac{\rho_p\gamma_p}{\rho_f\gamma_f}]G_r\{16(R(z)^2(\ln r - \ln \frac{R_c}{R_0})) \\ +r^2(1 + \ln R(z) - \ln r)(-\ln R(z) + \ln R_c/R_0) \\ +(\ln R(z) - \ln r)(1 + \ln R(z) - \ln R_c/R_0)(\frac{R_c}{R_o})^2\} \\ \frac{1}{64(\ln R(z)-\ln R_c/R_0)^2} + h[\frac{k_p+(n-1)k_f-(k_p-k_f)\phi}{k_p+(n-1)k_f+(n-1)(k_p-k_f)\phi}] \\ (r^4(\ln R(z))^2 + (R(z)^2 - r^2)\ln R_c/R_0)(4R(z)^2 + (3R(z)^2 - r^2)\ln R_c/R_0) \\ +R(z)^2\ln r(-4R(z)^2 + (-3R(z)^2 + 4r^2)\ln\frac{R_c}{R_0}) + \ln R(z)(4R(z)^2r^2 + \\ R(z)^2(3R(z)^2 - 4r^2)\ln r + (-3R(z)^4 + 4R(z)^2r^2 - 2r^4)\ln R_c/R_0) \\ -4(r^2(\ln R(z))^2 - 2R(z)^2\ln r + (R(z)^2 - r^2 + r^2\ln r)\ln R_c/R_0 + \\ \ln R(z)(R(z)^2 + r^2 - r^2(\ln r + \ln R_c/R_0))(R_c/R_0)^2 + (\ln R(z) - \ln r) \\ (4 + 3\ln R(z) - 3\ln R_c/R_0)(R_c/R_0)^4)) - \frac{(-\ln r+\ln R_c/R_0)u_B}{(\ln R(z)-\ln R_c/R_0)} \end{cases} \tag{3.1.2}$$

The volumetric flow rate Q is defined as:-

$$Q = \int_{R_c}^{R(z)} 2\pi r u du \tag{3.1.3}$$

$$Q = 2\pi\frac{dp}{dz}\frac{q_1(z)}{(\log R(z) - \log R_c)^2 - q_2(z)} \tag{3.1.4}$$

3.2. Numerical solution using finite difference method Finite difference method is employed for solution through numerical method. Denote u_i^k as the value of u at node r_i or z_i. In this notation, the finite difference formulation of various partial derivatives are given as:-

$$\frac{\partial u}{\partial r} \cong \frac{u_{i+1}^k - u_{i-1}^k}{2\Delta r} = u_r \tag{3.2.1}$$

$$\frac{\partial^2 u}{\partial^2 r} \cong \frac{u_{i+1}^k - 2u_i^k + u_{i-1}^k}{(\Delta r)^2} = u_{rr} \tag{3.2.2}$$

$$\frac{\partial \theta}{\partial r} \cong \frac{\theta_{i+1}^k - \theta_{I+1}^k}{2\Delta r} = \theta_r \tag{3.2.3}$$

$$\frac{\partial^2 \theta}{\partial r^2} \cong \frac{\theta_{i+1}^k - 2\theta_i^k + \theta_{i-1}^k}{(\Delta r)^2} = \theta_{rr} \tag{3.2.4}$$

$$\frac{\partial p}{\partial z} \cong \frac{p_{i+1-p_{i-1}^k}^k}{2\Delta z} = p_z \tag{3.2.5}$$

$$\frac{\partial p}{\partial r} \cong \frac{p_{i+1-p_{i-1}^k}^k}{2\Delta z} = p_r \tag{3.2.6}$$

The governing equations (2.23) to (2.25) are as follows:-

$$\frac{u^k i+1-u^k i-1}{2\Delta z}=0 \tag{3.2.7}$$

$$\frac{p^k i+1-p^k i-1}{2(\Delta r)}=0 \tag{3.2.8}$$

$$\begin{aligned}\frac{p^j i+1-p^j i-1}{2(\Delta z)}\frac{\mu_f}{\mu_{nf}}=\frac{u^k_{i+1}-2u^k_i+u^k_{i-1}}{(\Delta r)^2}+\frac{1}{r}\frac{u^k i+1-u^k i-1}{2\Delta r}\\ +[(1-\phi)+\phi\frac{\rho_p\gamma_p}{\rho_f\gamma_f}](1+A_1\phi+A_2\phi^2)G_r\theta\end{aligned} \tag{3.2.9}$$

$$\frac{\theta^k_{i+1}-2\theta^k_i+\theta^k_{i-1}}{(\Delta r)^2}+\frac{1}{r}\frac{\theta^k_{i+1}-\theta^k_{I+1}}{2\Delta r}+h[\frac{k_p+(n-1)k_f-(k_p-k_f)\phi}{k_p+(n-1)k_f+(n-1)(k_p-k_f)\phi}] \tag{3.2.10}$$

$$\theta^k_i=0 \quad at \quad r_i=R(z_i) \tag{3.2.11}$$

$$\theta^k_i=1 \quad at \quad r_i=\frac{R_c}{R_0} \tag{3.2.12}$$

$$u^k_i=u_b \quad at \quad r_i=R(z_i) \tag{3.2.13}$$

$$\frac{u^k i+1-u^k i-1}{2\Delta r}=\frac{\alpha}{\sqrt{Da}}(u_b-u_a) \tag{3.2.14}$$

The algorithm for solving the equations is given as:-

1. The radial domain is represented by a mesh of (n+1) grid points $0=r_0<r_1<r_2<\ldots\ldots\ldots\ldots\ldots<r_{n-1}<r_n=1$.
2. We seek the solution of θ and u at the mesh points for their respective regions.
3. The difference equations (3.2.7) to (3.2.10) and boundary conditions (3.2.11) to (3.2.14) are used to obtain the values at each grid point applying Thomas algorithm for tridiagonal system of matrices.

3.3. Comparison of analytical and numerical method Table 1 lists the values of u and θ obtained analytically and numerically and their corresponding errors.

$$n=8.6, \phi=0.02, h=2.0, Gr=2.0, Da=0.1, \delta=0.01, Rc/R_0=0.1$$

r	u (analytical)	u (numerical)	Error in u	θ (analytical)	θ (numerical)	Error in θ
0.1	0	0	0	1	1	0
0.2	1.990955	1.990734	0.000221	1.082149	1.081987	0.000162
0.3	2.909471	2.909125	0.000346	1.083809	1.083631	0.000178
0.4	3.293124	3.292590	0.000534	1.035628	1.035427	0.000201
0.5	3.313416	3.312980	0.000436	0.947211	0.946977	0.000234
0.6	3.046656	3.046225	0.000431	0.822838	0.822683	0.000155
0.7	2.533457	2.533081	0.000376	0.664789	0.664622	0.000167
0.8	1.797967	1.797626	0.000341	0.474427	0.472697	0.000173
0.9	0.855659	0.855429	0.000230	0.252630	0.252502	0.000128
1.0	0	0	0	0	0	0

TABLE 1.

3.4. Existence and uniqueness of analytical solution using Green's theorem Green's functions serve as important mathematical tools for explaining many physical concepts. These functions are of fundamental importance in understanding the theory of differential equations. The equations under consideration are (2.23) to (2.25). The solution depends on p, v and θ. (2.25) is a second order non-linear equation; considering only its leading term $\Theta^2 = 0$, which is a simple equation.

We divide the interval $0 \leq z \leq R(z)$ into n sub-intervals by the points $\eta_0 = 0, \eta_1, \eta_2, \ldots . \eta_n = R_a$ such that $\Delta\eta_i = \eta_i - \eta_{i-1}$. At some i, the corresponding $\eta_i = R_c$, where the point of jump discontinuity occurs. Let this be names as η. Let s be defined as $z/R(z)$ then $0 \leq s \leq 1$. Therefore the boundary conditions change to:-

$$\Theta = 0 \ \ at \ \ r = s \tag{3.4.1}$$

$$\Theta = 1 \ \ at \ \ r = s\eta \tag{3.4.2}$$

and the corresponding equation is

$$\Theta^2 = 0 \tag{3.4.3}$$

The corresponding Green's function is:-

$$G(\eta, s) = \begin{cases} (1-s)\eta & 0 \leq \eta \leq s \\ (1-\eta)\, s & s \leq \eta \leq 1 \end{cases} \tag{3.4.4}$$

Lemma 1:- If $\Theta(\eta) \, \epsilon \, C^2[0,1]$ satisfies the equation (3.4.1) to (3.4.2) then $|\Theta^k(\eta)| \leq C_k M, k = 0, 1$ where $M = max_{\eta\epsilon}[0,1]|\Theta^2(\eta)|$ and $C_0 = 0.0055$ and $C_1 = 0.6250$. $B\epsilon C^2[0,1]$ with the following norm on Θ on B is taken as the Banach space:- $\|\Theta\|$ $max_{k\epsilon 0,1}(\frac{C_0}{C_k} \, max_{0\leq\eta\leq 1}|\Theta^k(\eta)|)$

$$\textbf{proof} - \quad \Theta(\eta) = \int_0^1 G(\eta, s)\Theta^2(s)ds \tag{3.4.5}$$

$$\Theta^k(\eta) = \int_0^1 \frac{\partial^k}{\partial\eta^k} G(\eta, s)\Theta^2(s)ds \tag{3.4.6}$$

$$Then \ \ |\Theta^k(\eta)| \leq M \, max_{\eta\epsilon[0,1]} \int_0^1 |\frac{\partial^k}{\partial\eta^k} G(\eta, s)|ds \tag{3.4.7}$$

$$\int_0^1 |G(\eta, s)|ds = \frac{1}{2}(\eta - \eta^2) = 0 \leq 0.0055 \tag{3.4.8}$$

$$\int_0^1 |\frac{\partial}{\partial\eta}(G(\eta, s))|ds = |\frac{1}{2} - \eta| = 0.5 \leq 0.6250 \tag{3.4.9}$$

Lemma 2:- Let us consider (2.25) as $\Theta^2(\eta) = F(\eta, \Theta, \Theta')$. Then the function F satisfies:-$|F(\eta, \Theta_0, \Theta_1) - F(\eta, h_0, h_1)| \leq \sum_{k=0}^{1} L_k|\Theta_k - h_k|$ on $[0,1]X \quad D$ where $D = ((\Theta_0, \Theta_1)\epsilon\Re^2) : |\Theta_k - P_2{}^k(y)| < \frac{C_k}{C_0}, 0 \leq y \leq 1, 0 \leq k \leq 1$, $P_2(\eta)$is a one degree

polynomial satisfying equations (3.4.8) and (3.4.9) and $L_k, k = 0, 2$ are constants.
proof:-Let $(\eta, \Theta_0, \Theta_1)$ and (η, h_0, h_1) are arbitrary in $[0, 1]X \quad D$. Then using mean value theorem, $\exists$ some $j_0, j_1 \ \epsilon \ D$ such that

$$F(\eta, \Theta_0, \Theta_1) - F(\eta, h_0, h_1) = \sum_{k=0}^{1} \frac{\partial F}{\partial \Theta_k}(j_k)(\Theta_k - h_k) \tag{3.4.10}$$

Now based on definition of F, its partial derivatives are calculated as

$$\frac{\partial F}{\partial \Theta_0} = 1, \frac{\partial F}{\partial \Theta_1} = \eta \tag{3.4.11}$$

$$It\ is\ easy\ to\ see\ that\ P_2(\eta) = \frac{1}{2}\eta \tag{3.4.12}$$

Therefore, based on the definition of D, the following required inequalities holds:-

$$|\frac{\partial F}{\partial \Theta_1}| = |\eta| \leq 1 \leq 1.1924 \tag{3.4.13}$$

$$|\frac{\partial F}{\partial \Theta_0}| = |1| \leq 116.64 \tag{3.4.14}$$

Therefore, the equation $T|F(\eta, \Theta_0, \Theta_1) - F(\eta, h_0, h_1)| \leq \sum_{k=0}^{1} L_k|\Theta_k - h_k|$ holds with

$$L_0 = 116.64, \quad L_1 = 1.1924 \tag{3.4.15}$$

Theorem:- If $L_0C_0 + L_1C_1 < 1$, then there exists a unique pair of solution of $[\Theta(\eta)]$ for the equations (2.25) with equations (2.27) and (2.28) as boundary conditions.

proof:-First, the existence of f will be proved. Let us define the operator

$$T : K(P_2(\eta), 1) \subset B \to B \ \ as\ follows : -$$

$$T(\Theta(\eta)) = P_2(\eta) + \int_0^1 G(\eta, s)(F(s, f(s), f'(s))ds \tag{3.4.16}$$

Therefore $T^2(\Theta(\eta)) = F(\eta, \Theta(\eta), \Theta'(\eta))$ and $T(\Theta(\eta))$satisfies the boundary conditions (3.4.8) and (3.4.9). Now if T has a fixed point that is $T(\Theta) = \Theta$ then Θ will be the solution of the problem given from (2.25). Therefore, if suffices to prove the existence of a fixed point. Let $\Theta(\eta)$, $h(\eta)\epsilon K(P_2(\eta), 1)$, then:-

$$T(\Theta^k(\eta)) - T(h^k(\eta)) = \int_0^1 G(\eta, s)[F(s, \Theta(s), \Theta'(s) - F(s, h(s), h'(s)]ds \tag{3.4.17}$$

Now by Lemma 1 and Lemma 2, we have:-

$$|T(\Theta^k(\eta)) - T(h^k(\eta))| \leq C_k max_{0\leq s\leq 1}|T(\Theta^2(s) - T(h^2(s)| \tag{3.4.18}$$

$$\leq C_k max_{0\leq s\leq 1} \sum_{j=0}^{1} L_j|\Theta^j(s) - h^j(s)| \tag{3.4.19}$$

$$\leq C_k \sum_{j=0}^{1} L_j \frac{C_j}{C_0} \|\Theta - h\| \tag{3.4.20}$$

$$Therefore \ \ \|T(\Theta) - T(h)\| \ \leq \ l\|(\Theta - h)\| \tag{3.4.21}$$

Therefore is a contraction mapping on $K(P_2(\eta, 1)$ and then using Lemma 2.3 of Agarwal and Chow [36], it has a unique fixed point that is the solution of equations (2.25) and (2.27), (2.28).

4. Graphical results and discussions

This mathematical analysis for the flow of different shapes of nanoparticles in a catheterized artery with elliptical stenosis is taken into account parameters like shape factor n , A_1 and A_2, catheter radius R_c, volume fraction ϕ of nanoparticles, heat source parameter h, Grashof number Gr , stenosis depth δ and Darcy number Da on temperature and velocity of nanofluid. The graphs are plotted using MATLAB. Fig 2-5 depicts temperature of nanofluid for shape parameter n,A_1 and A_2 , catheter radius R_c, volume fraction ϕ, and heat source parameter h. Fig 6-12 exhibits axial velocity of nanofluid for shape parameter n,A_1 and A_2 ,catheter radius R_c, volume fraction ϕ, heat source parameter h, Grashof number Gr, stenosis depth δ, and Darcy number Da.

Figure 2 shows the temperature θ of nanofluid versus radial direction r for distinct values of shape parameters n ,A_1 and A_2. The trend in general is parabolic because of uptrend in the temperature with the increase in radial distance. Shape parameter is the measure of ratio of equal volumes of real particle's surface area to sphere's surface area. Shape factor is an important pharmocological property of a drug. It effects the release of a drug, its absorption and subsequently its therapeutic action. Higher shape factor has interaction the interaction of the given shape of nanoparticle with the fluid interface, thus higher the viscosity. Thus, platelet shaped nanoparticles show least viscosity because of greatest shape factor. Similar results were given by Ijaz and Nadeem [6], Devaki et al [38] and Madhura et al [28]. Also, some of the experimental studies on different shapes of nanoparticles have shown similar results [29].

Figure 3 displays the graph of temperature θ of nanofluid versus radial direction r for different values of catheter radius R_c for brick shaped nanoparticles. Catheters provide continuous hemodynamic monitoring along with clearing the occlusions.The radius of the catheter used effects the stables securement of the catheter. The trend shows that the temperature increases with the increase in catheter radius. The frictional resistance increases with the increasing radius of catheter. Thus, the resistance to flow increases which raises the temperature [40].

Figure 4 depicts the variation of temperature θ of nanofluid versus radial direction r for different values of volume fraction ϕ of brick shaped nanoparticles. Volume fraction represents the number of nanoparticles dispersed in blood. The increase in volume

fraction for nanoparticles causes an increase in the number of nanoparticles in blood. The increase in number of nanoparticles causes a greater increase in the transportation of nanoparticles via conduction from catheter wall to the artery wall with raises the temperature of nanofluid. Thus, the rise in volume fraction of nanoparticles, raises temperature of nanofluid. Similar results were given by Nayak et al [41]. The results are in accordance with the experimental study by Timofeeva et al [29].

Figure 5 displays temperature θ of nanofluid versus radial direction r for different values of heat source parameter h for brick shaped nanoparticles. Heat source parameter governs the temperature. As the value of heat source parameter grows it brings an elevation in heat generation which raises the temperature of nanofluid. Thus, the graph shows a rise in temperature with enhancement in heat source parameter. Similar results were given by Ijaz and Nadeem [6] for spherical shaped nanoparticles.

Figure 6 exhibits velocity u versus radial direction r for different shapes of nanoparticles. The trend is parabolic in general because velocity is changing at a constant rate with respect to radius.Monitoring the shape of nanoparticles is of paramount importance in pharmocology.Shape factor determines the degree of effectiveness of the drug indirectly by controlling its interaction with the blood cells,their dissolution rate and bio-availabilty. Brick shaped nanoparticles in blood show least velocity profile while platelet shaped nanoparticles show highest velocity profile. The consequence of the shape of nanoparticles on the velocity is because of the viscosity dependence-relation of the shape of respective nanoparticle at a given temperature. Brick shaped nanoparticles show maximum viscosity while platelet shaped nanoparticles have least viscosity.Similar observations were reported by Nayak et al[41].The results are in agreement with the experimental results obtained by Timofeeva et al [29].

Figure 7 depicts velocity u versus radial direction r using distinct values of catheter radius R_c with brick shaped nanoparticles in nanofluid. The velocity rises with the increase in catheter radius to occupy for the same volume of fluid flowing in the diseased artery [40].The flow is inversely proportional to the viscosity as stated by Poiseuille's law.This result can be applied for cleaning of blockages with a suitable radius of catheter.

Figure 8 depicts velocity u versus radial direction r using distinct values of volume fraction ϕ of brick shaped nanoparticles. The velocity decreases with rise in the value of volume fraction of nanoparticles.Volume fraction of nanoparticles is the indication of concentration of nanoparticle present. The reason is attributed to the fact that as the volume fraction increases, the number of nanoparticles increases, which causes the nanofluid to become more viscous. The rise in viscosity causes a rise in friction force which reduces velocity. Similar experimental results for drug delivery in a catheterized artery with atherosclerosis was given by Orizaga et al [39].

Figure 9 exhibits velocity u versus radial direction r for different values of heat source parameter h for brick shaped nanoparticles. The rise in heat source parameter causes a rise in temperature which decreases the viscosity, thereby increasing the velocity. Devaki et al [38] and Ijaz and Nadeem [6] gave comparable results.

Figure 10 shows velocity u versus radial direction r for distinct values of Grashof number Gr for brick shaped nanoparticles. The results show that velocity rises with the rise in the value of Grashof number. Grashof number is the ratio of upthrust by fluid density because of temperature difference to restraining forces because of viscosity of nanofluid. The increase in value of Grashof number reduces the viscosity of the nanofluid which thus increases the velocity. Similar analysis has been given by Devaki et al [38].

Fig 11 shows velocity u versus radial direction r for distinct values of stenosis depth δ for brick shaped nanoparticles. The trend shows that velocity increases with increase in stenosis depth. This is because the nanofluid moves more rapidly in the same volume. Thus, the increases in velocity at the stenosis is proportional to the thickness of the blockage occurred.

Figure 12 exhibits velocity u versus radial direction r using different values of Darcy number Da for brick shaped nanoparticles. Darcy number represents the relative effect of the permeability of the medium to its cross-sectional area. The trend shows that the increase in the value of Darcy number decreases the velocity of the nanofluid. This is because the increase in the permeability causes a decrease in the velocity of the nanofluid [6].

5. Conclusions

The flow of a nanofluid is theoretically examined in elliptical stenosed artery with a catheter with gold nanoparticles. The governing equations were solved using Cauchy-Euler method. The graphs were plotted using MATLAB for temperature and axial velocity of nanofluid with respect to parameters like shape factor n , A_1 and A_2, catheter radius R_c, volume fraction ϕ of nanoparticles, heat source parameter h, Grashof number Gr , stenosis depth δ and Darcy number Da. The results established can be outlined as:-

1. The platelet shaped nanoparticles show maximum rise in temperature and velocity while brick shaped nanoparticles show least rise in temperature and velocity.
2. The temperature of nanofluid increases with increase in catheter radius, volume fraction and heat source parameter.
3. The velocity of nanofluid increases with increase in catheter radius, Grashof number, stenosis depth and heat source parameter while it decreases with increase in volume fraction and Darcy number.

From the above results it can be concluded that the shape of the nanoparticle can be designated relying on their application and their respective thermodynamic properties can be administered. The above model can be further developed for full vasculature taking into account nanoparticle clustering. It is hoped that the developed mathematical model has efficacious application in the therapeutics dealing with cardiovascular diseases.

6. Appendix

The thermophysical properties of the blood [19] are:-

C_p	3594 J/KgK
ρ	1063 Kg/m^3
k	0.492 W/mK
γ	$0.18x10^{-}5$ 1/K

Table 2.

The values of shape factor of nanoparticles[28] are:-

Shape Of nanoparticle	η	A_1	A_2
Platelets	5.7	37.1	612.6
Blades	8.6	14.6	123.3
Cylinders	4.9	13.5	904.4
Bricks	3.7	1.9	471.4

Table 3.

$$\begin{cases} q_1(z) = ((logR(z) - logR_c))^2(4R(z)\alpha Da((R(z))^2(1 - 2R(z) + 2logR_c) - R_c^2) \\ + \sqrt{Da}((R(z))^4(-3 + 4logR(z) - 4logR_c) + 49R(z))^2R_c^2 \\ -R_c^4) + R(z)\alpha((R(z))^4(1 - logR(z) + logR_c) \\ -2(R(z))^2R_c^2 + (1 + logR(z) - logR_c)R_c^4)) \\ /(16/(1 + A\phi)(R(z)\alpha(logR(z) - logR_c) - \sqrt{Da})) \end{cases} \tag{6.0.1}$$

$$
\begin{cases}
q_2(z) = ((logR(z) - logR_c))^2(2R(z)\alpha(6((R(z))^4(-4 + 3logR(z) - 3logR_c) \\
+4(R(z))^2(2 + logR(z) - logR_c)R_c^2 - (4 + 7logR(z) + 4(logR(z))^2 \\
-(7 + 8logR(z))logR_c \\
+4((logR_c))^2)R_c^4) + 2h[\frac{k_p+(n-1)k_f-(k_p-k_f)\phi}{k_p+(n-1)k_f+(n-1)(k_p-k_f)\phi}]((R(z))^2 - R_c^2) \\
((R(z))^4(6 - 9logR(z) + 4logR(z))^2 + (9 - 8logR(z))logR_c \\
+4((logR_c))^2) + 4(R(z))^2(-3 + ((logR(z) - logR_c))^2)R_c^2 \\
+(6 + 9logR(z) + 4logR(z))^2 - (9 + 8logR(z))logR_c \\
+4((logR_c))^2)R_c^4) + \sqrt{Da}(12((R(z))^4(9 - 8logR(z) + 8logR_c) \\
-4(R(z))^2)(3 + 2logR(z) - 2logR_c)((logR_c))^2(3 + 4logR(z) - 4logR_c) \\
((logR_c))^4) + h[\frac{k_p+(n-1)k_f-(k_p-k_f)\phi}{k_p+(n-1)k_f+(n-1)(k_p-k_f)\phi}] \\
(-(R(z))^6(27 - 46logR(z) + 24(logR(z))^2 \\
+2(23 - 24logR(z)logR_c + 24logR_c)^2) + 9(R(z))^4(7 - 4logR(z) \\
+4logR_c)R_c^2 - 9(R(z))^2(5 + 2logR(z) - 2logR_c)R_c^4 \\
+(9 + 8logR(z) - 8logR_c)R_c^6)))) \\
/(768(logR(z) - logR_c))(R(z)\alpha(logR(z) - logR_c) - \sqrt{Da}))
\end{cases}
\tag{6.0.2}
$$

Author contributions:
Conceptualization: R Bali, B Prasad ; *Software*: B Prasad; *Writing-Original Draft:* B Prasad

Conflicts of interest: The authors declare that there are no conflicts of interest.

Funding statement: This research did not receive any specific grant from funding agencies in the public, commercial, or not-for-profit sectors.

References

[1] S Nadeem and S Ijaz. *Nanoparticles analysis on the blood flow through a tapered catheterized elastic artery with overlapping stenosis, The European Physical Journal Plus (2014) 129:249 DOI-10.1140/epjp/i2014-14249-1*

[2] S Chakravarty and A Datta. *Effects of stenosis on arterial rheology through a mathematical model,* Mathematical and Computer Modelling **12** (1989): 1601-1612 DOI:-10.1016 / 0895-7177(89)90336-1

[3] D N Ku. *Blood flow in arteries,* Ann. Rev Fluid Mech. Vol **29**, (1997) pp:399-434

[4] Akbar Zaman, Nasir Ali, O. Anwar Beg. *Numerical simulation of unsteady micropolar hemodynamics in a tapered catheterized artery with a combination of stenosis and aneurysm,* Med Biol Eng Comput **54**(2016):1423-1436

[5] S Mishra, S U Siddiqui, A Medhavi. *Blood flow through a composite stenosis in an artery with permeable wall,* Int J Appl Appl Maths **6** (2011) 58-73

[6] S Ijaz and S Nadeem. *Examination of nanoparticles as a drug carrier on blood flow through a catheterized composite stenosed artery with permeable walls,* Computer methods and programs in biomedicine **133** (2016) pg-83-94 DOI-10.1016/j.cmpb.2016.05.004

[7] K S Mekheimer, M A El Kot. *Suspension model for blood flow through arterial catheterization,* Chem Eng Comm **197** (2010) 1195-1214

[8] N K Verma, S Mishra, S U Siddiqui, R S Gupta.*Study of blood flow through a catheterized artery,* Adv Appl Sci Res **2** (2011) 114-122

[9] R K Srivastav. *Mathematical model of blood flow through a composite stenosis in catheterized artery with permeable wall,* Appl Maths (2007) **99**, 58-74

[10] V P Srivastava, R Srivastava. *Particulate suspension blood flow through a narrow-catheterized artery,* Comput Math Appl (2009) **58**, 227-238

[11] I Khan, K Saeed, I Khan. *Review- Nanoparticles: Properties, applications, and toxicities,* Arabian Journal of Chemistry (2017),**12**, 908-931 DOI-10.1016/j.arabjc.2017.05.011

[12] R Ellahi, S U Rahman, M Gulzar, S Nadeem, K Vafai.*A mathematical study of non-Newtonian micropolar fluid in arterial blood flow through composite stenosis,* Appl Math Inf Sci (2014)**4**,1567-1573

[13] Sarafaraz Kamangar, Govindaraju Kalimuthu, Irfan Anjum Badruddin, A Badarudin, N J Salman Ahmed, T M Yunus Khan.*Numerical investigation of the effect of stenosis geometry on the coronary diagnostic parameters,* The Scientific World Journal, Hindawi Publication. (2014) ,**354946**, DOI:10.1155/2014/354946

[14] Rekha Bali, Bhawini Prasad, Swati Mishra.*A Review On Mathematical Models For Nanoparticle Delivery In The Blood.* International Journal of Advanced Research (IJAR) (2020),**10**(04) Article DOI:10.21474/IJAR01/14526, 130-146, ISSN:2320-5407

[15] G Sangeetha, N Usha, R Nandini, P Kaveya, G Vidhya, B Chaithanya.*A review on properties, applications and toxicities of metal nanoparticles,* International Journal of Applied Pharmaceutics (2020) Vol **12**, Issue 5, DOI- 10.22159/ijap.2020v1215.3874

[16] S U S Choi.*Enhancing thermal conductivity of fluids with nanoparticles in : D A Siginer, H P Wang (Eds), Developments and Applications of Non-Newtonian flows,* ASME (1995), pp 99-105.36

[17] R X Yin, D Z Yang, J Z Wu. *Nanoparticle drug and gene-eluting stents for the prevention and treatment of coronary restenosis,* Theranostics (2014),**4**, 175-200

[18] P Rajashekharreddy, V T Anju, M Dyavaiah, B Siddhardha, M S Nauli. *Nanoparticle mediated drug delivery for the treatment of cardiovascular diseases,* International Journal of Nanomedicine (2020)**15**, 3741-3769 DOI-10.2147/IJN.5250872

[19] R Ellahi, S U Rahman, S Nadeem, N S Akbar.*Blood flow of nanofluid through an artery with composite stenosis and permeable walls,* Appl Nanosci (2014),**4**, 919-926

[20] S Nadeem and S Ijaz. *Theoretical examination of metallic nanoparticles on blood flow through stenosed artery with permeable walls.* Phys Lett A (2015)**379**, 542-554

[21] S Nadeem and S Ijaz. *Theoretical examination of nanoparticles as a drug carrier with slip effects on the wall of stenosed arteries,* Int J Heat Mass Transf (2016)**93**, 1137-1149

[22] A Chatterjee, S Changdar, S De. Study of nanoparticle as a drug carrier through stenosed arteries using Bernstien polynomials, International Journal for Computational Methods in Engineering Science and Mechanics. (2020) DOI:-10.1080/15502287.2020.1821125

[23] S Rathore and D Srikanth. Mathematical study of transport phenomena of blood nanofluid in a diseased artery subject to catheterization. Indian J Phys.(2021) DOI:-10.1007/s12648-021-02166-2

[24] Goncalves, R Souza, G Coutinho, J Mirando, A Moita, J E Pereira, A Moreira, R Lima.*Thermal conductivity of nanofluids: A review on prediction models, controversies and challenges.* Applied Sciences (2021) **11**, 2525 DOI-10.3390/apps11062525

[25] S Simpson, A Schelfhout, C Golden, S Vafai. *Nanofluid thermal conductivity and effective parameters.* Applied Science (2019) **9**, 87 DOI-10.3390/app9010087

[26] D R V S R K Sastry, N N Kumar, P K Kameswaran, Sachin Shaw.*Unsteady 3D micropolar nanofluid flow through a squeezing channel: application to cardiovascular disorders.* Indian Journal of Physics, (2022)**96** 57-70 DOI:10.1007/s12648-020-04951-9

[27] Annah J Moitoi, Sachin Shaw.*Magnetic drug targeting during Caputo-Fabrizio fractionalised blood flow through a permeable vessel.* Microvascular Research, (2022)**139** 104262 DOI:10.1016/j.mvr.2021.104262

[28] K R Madhura, B Atiwali, S S Iyengar. Influence of nanoparticle shapes on natural convection flow with heat and mass transfer rates of nanofluids with fractional derivative. Math Meth Appl Sci (2021); 1-17 DOI-10.1002/mma.7404

[29] E V Timofeeva, J L Routbost, D Singh.*Particle shape effects on thermophysical properties of alumina nanofluids,* Journal of applied physics (2009),**106**, 014304 DOI- 10.1063/1.3155999

[30] S S Samantray, Sachin Shaw, A Mishra, M K Nayak, J Prakash. *Darcy-Forchheimer up/down flow of entropy optimised radiative nanofluid with second order slip, non uniform source/sink and shape effects,* Heat Transfer, (2022) ,**51**, 2318-2342 DOI:10.1002/htj.22403

[31] Sachin Shaw, G C Shit, D Tripathi.*Impact of drug carrier shape, size, porosity and blood rheology on magnetic nanoparticle based drug delivery in a microvessel,* Colloids and Surfaces A:Physicochemical and Engineering Aspects, (2022),**639** 128370, DOI:10.1016/j.colsurfa.2022.128370

[32] R Narayana. *Nanoparticles of different shapes for biosensor applications,* ACS Symp Ser (2012) **1112** : 281-292

[33] L Qiu, N Zh, Y Feng, E E Michaelides, G Zyla, D Jing, X Chang, P M Norris, C N Markides, O Mahian.*A review of recent advances in thermophysical properties at the nanoscale: from solid state to colloids,* Physics Reports (2020) **843**,1-81 DOI-10.1016/j.physrep.2019.12.001

[34] R Ellahi, M Hassan, A Zeeshan.*Shape effects of nanosize particles in Cu-H2O nanofluid on entropy generation,* Int J Heat Mass Transf (2015)**81** ,449-456

[35] J L Auriault.*About the Beavers and Joseph boundary condition,* Transport in porous media. Springer Science+Business Media B.V. (2009). DOI-10.1007/s11242-009-9435-9

[36] R P Agarwal, Y M Chow. *Iterative methods for a fourth order boundary value problem,* Journal of Computational and Applied Mathematics. (1984) Vol **10**, No. 2, pp 203-217

[37] M Esmaeili, H H Mehne, D D Ganji. *On the existence and uniqueness of solution for squeezing nanofluid flow problem and Green-Picard's iteration,* International Journal of Numerical Methods for Heat and Fluid Flow. (2020) 0961-5539 DOI:10.1108/HFF-07-2020-0427

[38] P Devaki, B Venkateswarlu, S Srinivas, S Sreenadh. MHD *Peristaltic flow of a nanofluid in a constricted artery for different shapes of nanosized particles,* Nonlinear Engineering 2020;**9** (2017) 51-59 DOI:10.1515/nleng-2017-0064

[39] S Orizaga, D N Riahi, J R Soto.*Drug delivery in catheterized arterial blood flow with atherosclerosis,* Results in Applied Mathematics.**7** (2020) 100117 DOI:10.1016/j.rinam.2020.10017

[40] D S Sankar, U Lee.*Two-fluid Herschel-Bulkley model for blood flow in catheterized arteries,* Journal of Mechanical Science and Technology **22** (2008) pp 1008-1018 DOI:10.1007/s12206-008-0123-4

[41] M K Nayak, Sachin Shaw, M I Khan, O D Makinde, Yu-Ming Chu, S U Khan. *Interfacial layer and shape effects of modified Hamilton's Crosser model in entropy optimised Darcy-Forchheimer flow,* Alexandria Engineering Journal, **60** (2021) 4067-4083 DOI:10.1016/j.aej.2021.02.010

R. Bali, Department of Mathematics, School of Basic and Applied Sciences, Harcourt Butler Technical University, Kanpur,India
e-mail: dr.rekhabali1965@ymail.com

B. Prasad, Department of Mathematics, School of Basic and Applied Sciences, Harcourt Butler Technical University, Kanpur,India
e-mail: jayabhawini@gmail.com

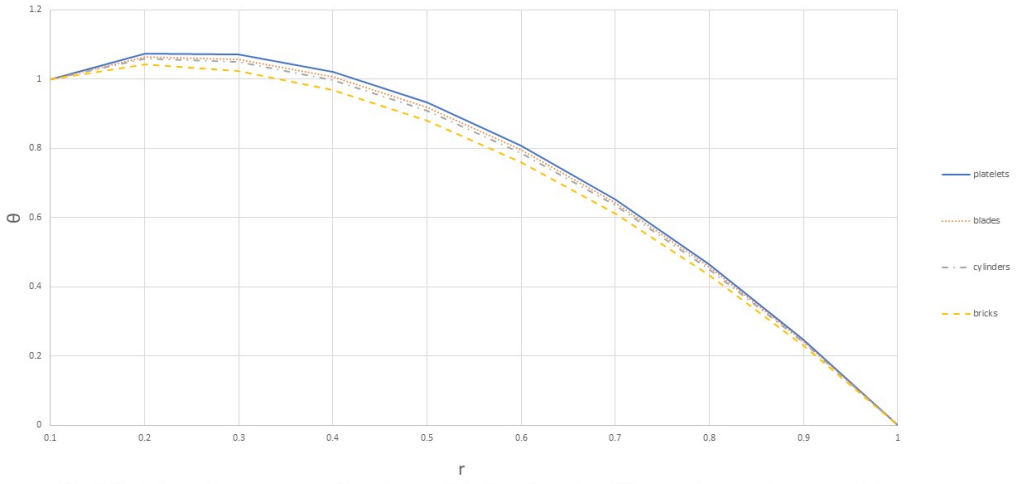

Fig 2 Variation of temperature θ against radial direction r for different shapes of nanoparticles Rc=0.1,ϕ =0.01,h=5.0

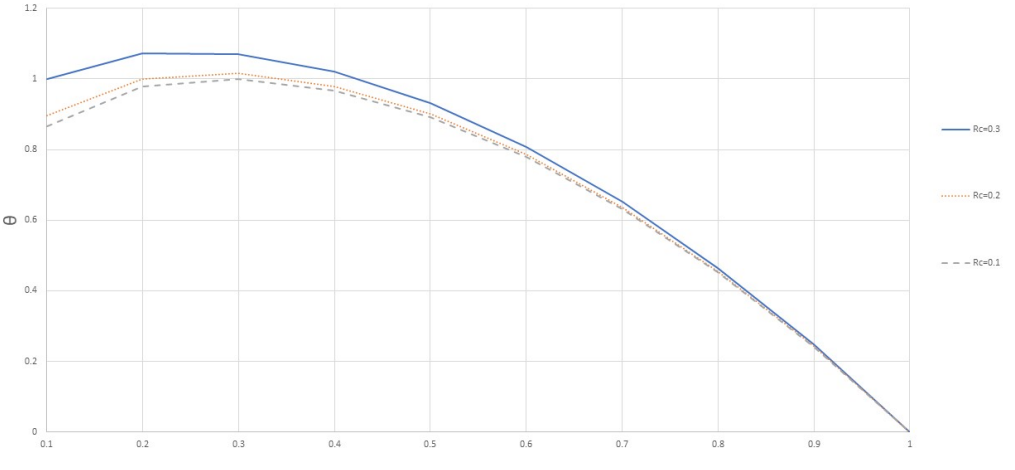

Fig 3 Variation of temperature θ against radial direction r for different values of catheter radius Rc n=3.7,ϕ =0.01,h=5.0

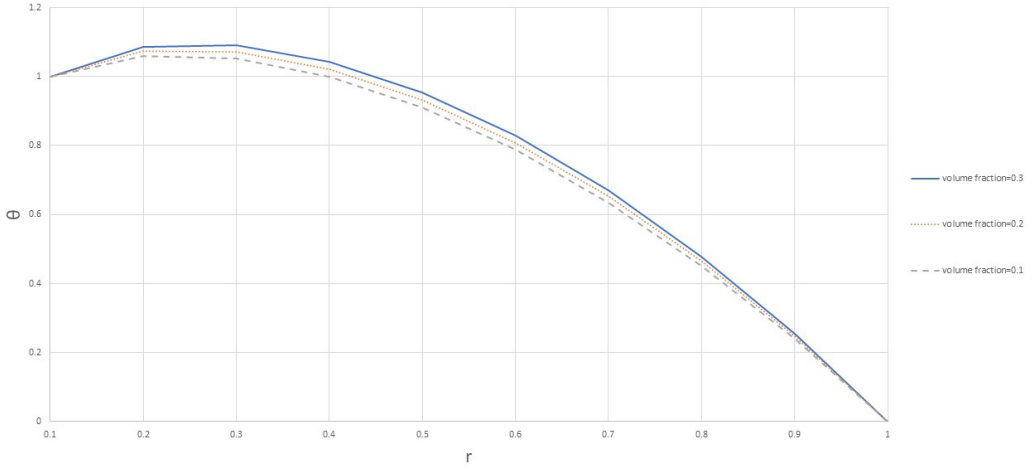

Fig 4 Variation of temperature θ against radial direction r for different values of volume fraction ϕ n=3.7,Rc =0.1,h=5.0

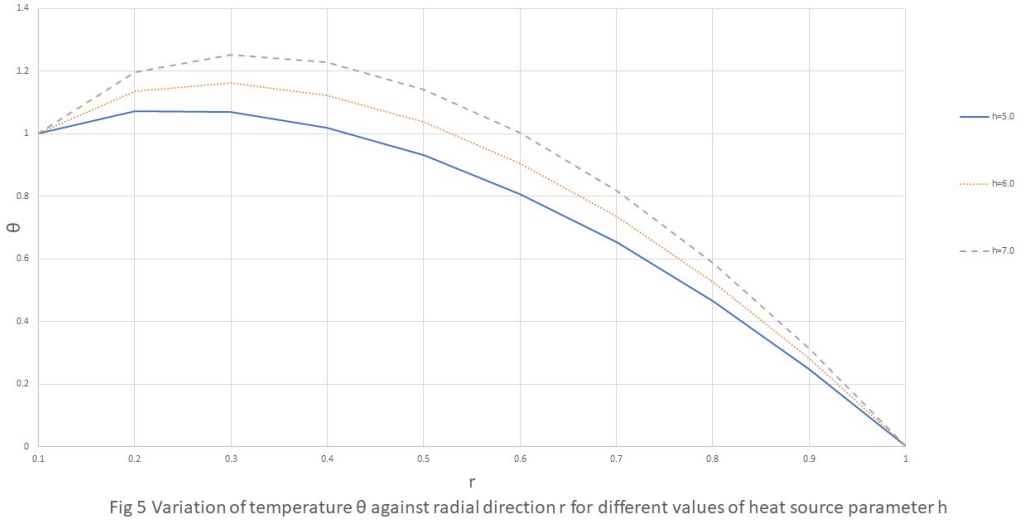

Fig 5 Variation of temperature θ against radial direction r for different values of heat source parameter h n=3.7,Rc=0.1, ϕ=0.01

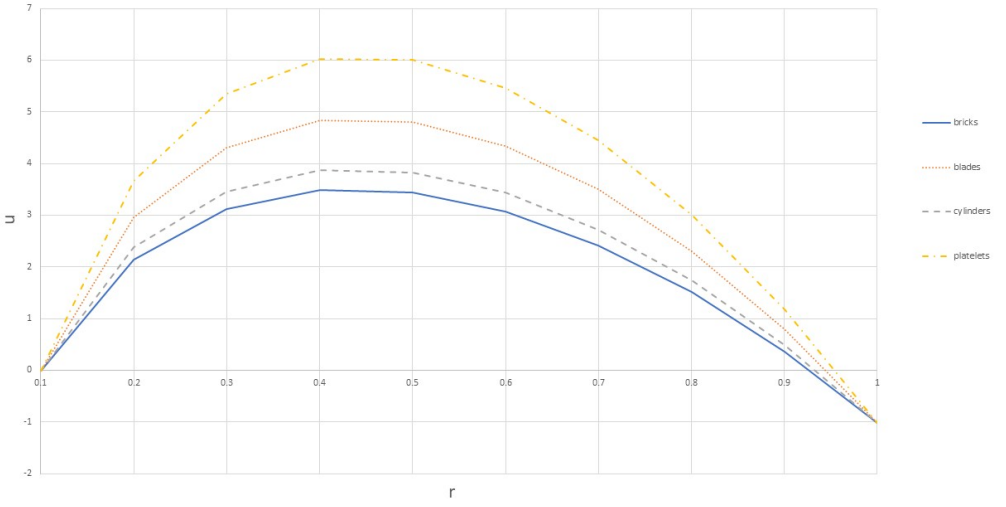

Fig 6 Variation of velocity u against radial direction r for different shapes of nanoparticles
Rc=0.1,ϕ =0.01, h=5.0,Gr=4.0, δ =0.1, Da=0.1

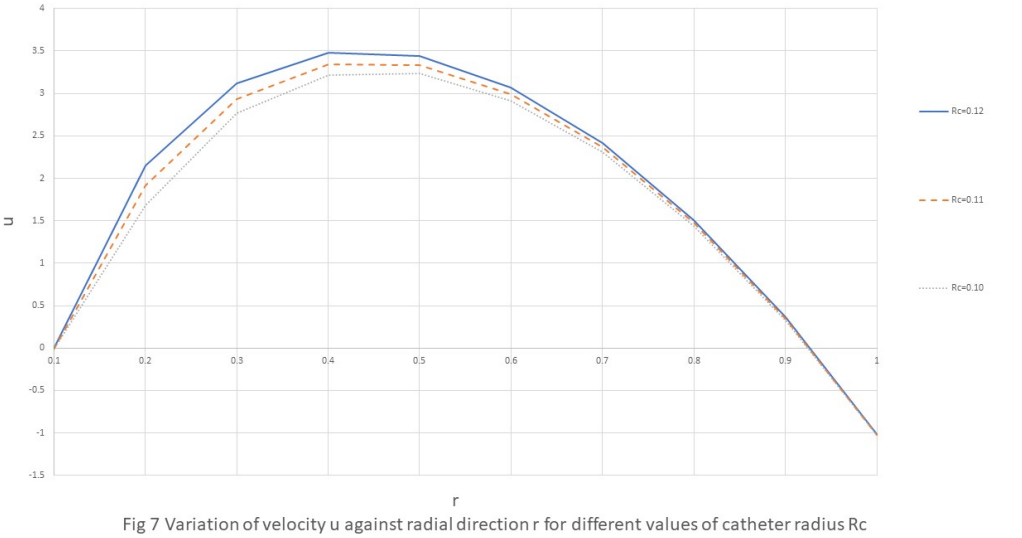

Fig 7 Variation of velocity u against radial direction r for different values of catheter radius Rc
n=3.7,ϕ =0.01, h=5.0,Gr=4.0, δ =0.1, Da=0.1

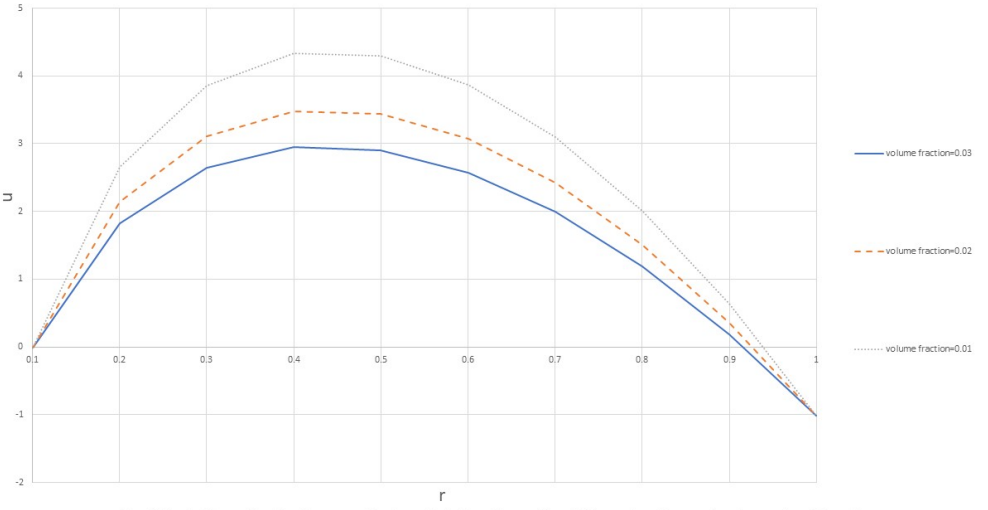

Fig 8 Variation of velocity u against radial direction r for different values of volume fraction ϕ n=3.7,Rc=0.1, h=5.0,Gr=4.0, δ =0.1, Da=0.1

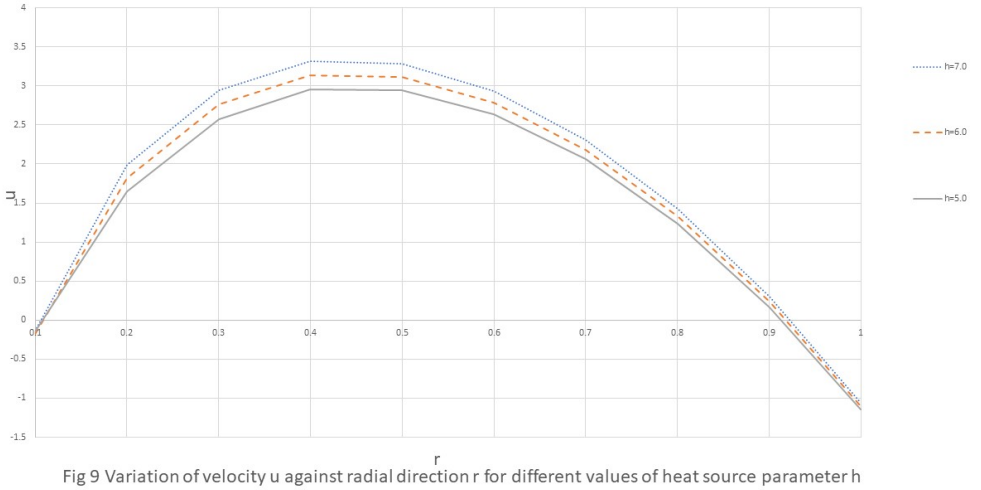

Fig 9 Variation of velocity u against radial direction r for different values of heat source parameter h Rc=0.1,ϕ =0.01, n=3.7,Gr=4.0, δ =0.1, Da=0.1

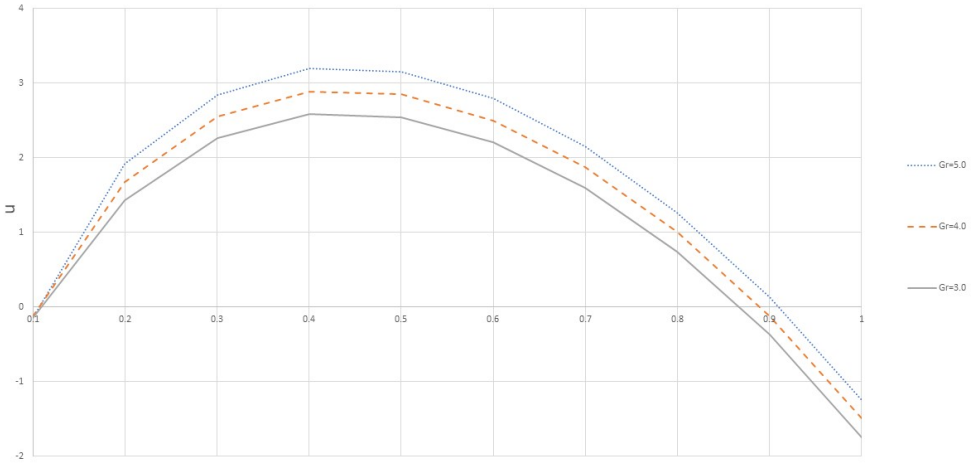

Fig 10 Variation of velocity u against radial direction r for different values of Grashof number Gr
Rc=0.1,ϕ =0.01, h=5.0,n=3.7, δ =0.1, Da=0.1

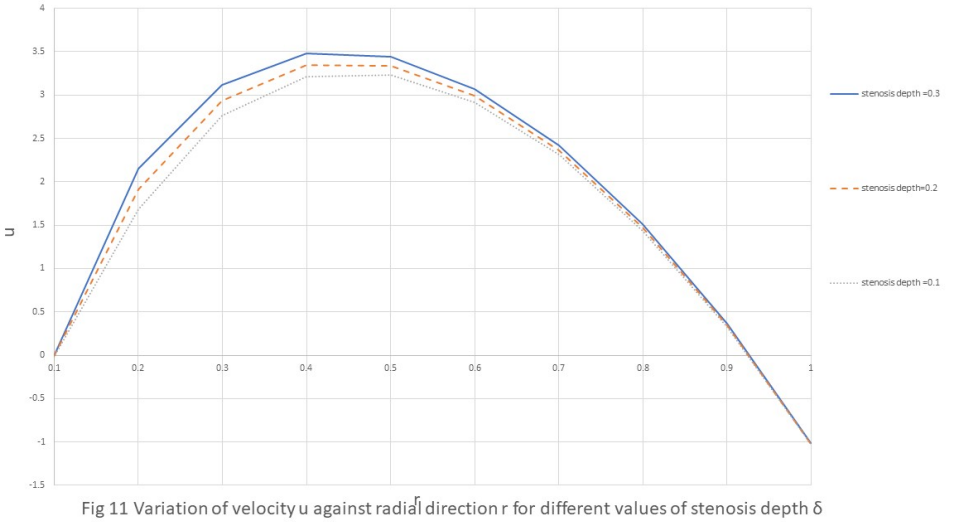

Fig 11 Variation of velocity u against radial direction r for different values of stenosis depth δ
Rc=0.1,ϕ =0.01, h=5.0,Gr=4.0, n=3.7, Da=0.1

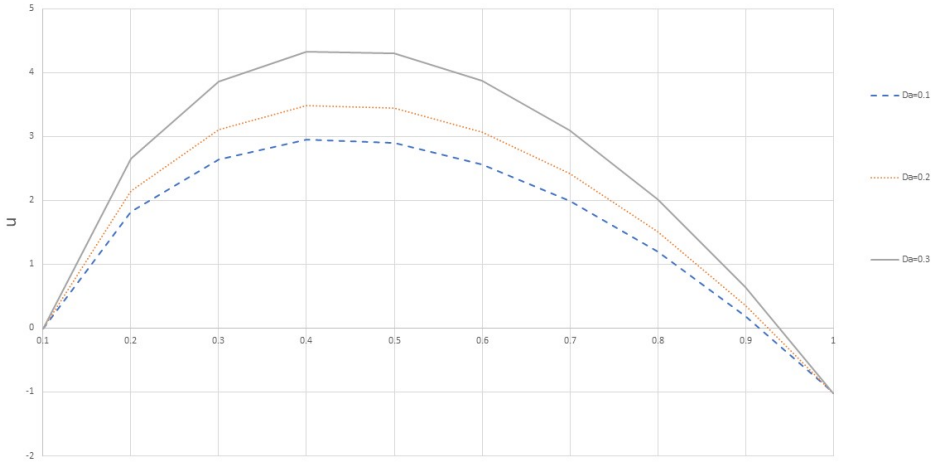

Fig 12 Variation of velocity u against radial direction r for different values of Darcy number Da Rc=0.1,ϕ =0.01, h=5.0,Gr=4.0, δ =0.1, n=3.7